NASA TECHNICAL NOTE

NASA TN D-7747

NASA TN D-7747

ANALYSIS AND COMPENSATION OF AN AIRCRAFT SIMULATOR CONTROL LOADING SYSTEM WITH COMPLIANT LINKAGE

by Paul R. Johansen and Richard E. Bardusch

Langley Research Center

Hampton, Va. 23665

NATIONAL AERONAUTICS AND SPACE ADMINISTRATION • WASHINGTON, D. C. • DECEMBER 1974

1. Report No.	2. Government Accession No.	3. Recipient's Catalog No.
NASA TN D-7747		

4. Title and Subtitle	5. Report Date
ANALYSIS AND COMPENSATION OF AN AIRCRAFT SIMULATOR CONTROL LOADING SYSTEM WITH COMPLIANT LINKAGE	December 1974
	6. Performing Organization Code
7. Author(s)	8. Performing Organization Report No.
Paul R. Johansen and Richard E. Bardusch	L-9642
	10. Work Unit No.
9. Performing Organization Name and Address	504-39-11-03
NASA Langley Research Center Hampton, Va. 23665	11. Contract or Grant No.
	13. Type of Report and Period Covered
12. Sponsoring Agency Name and Address	Technical Note
National Aeronautics and Space Administration Washington, D.C. 20546	14. Sponsoring Agency Code

15. Supplementary Notes

Paul R. Johansen is Assistant Professor of Mechanical Engineering, Iowa State University of Science and Technology, Ames, Iowa.

16. Abstract

A hydraulic control loading system for aircraft simulation was analyzed to find the causes of undesirable low frequency oscillations and loading effects in the output. The hypothesis of mechanical compliance in the control linkage was substantiated by comparing the behavior of a mathematical model of the system with previously obtained experimental data.

A compensation scheme based on the minimum integral of the squared difference between desired and actual output was shown to be effective in reducing the undesirable output effects. The structure of the proposed compensation was computed by use of a dynamic programing algorithm and a linear state space model of the fixed elements in the system.

17. Key Words (Suggested by Author(s))	18. Distribution Statement
Simulation Control systems Electrohydraulic servo Optimization by dynamic programing	Unclassified – Unlimited STAR Category 10

19. Security Classif. (of this report)	20. Security Classif. (of this page)	21. No. of Pages	22. Price*
Unclassified	Unclassified	29	$3.75

*For sale by the National Technical Information Service, Springfield, Virginia 22151

ANALYSIS AND COMPENSATION OF AN AIRCRAFT SIMULATOR CONTROL LOADING SYSTEM WITH COMPLIANT LINKAGE

By Paul R. Johansen* and Richard E. Bardusch
Langley Research Center

SUMMARY

A hydraulic control loading system for aircraft simulation was analyzed to find the causes of undesirable low frequency oscillations and loading effects in the output. The hypothesis of mechanical compliance in the control linkage was substantiated by comparing the behavior of a mathematical model of the system with previously obtained experimental data.

A compensation scheme based on the minimum integral of the squared difference between desired and actual output was shown to be effective in reducing the undesirable output effects. The structure of the proposed compensation was computed by use of a dynamic programing algorithm and a linear state space model of the fixed elements in the system.

INTRODUCTION

Control systems in aircraft which convert stick, wheel, and pedal motions into control surface deflections constitute the interface between pilot and airframe. In addition to the pilot input function, such systems provide force cues to the pilot which assist him in assessing the extent and rate of controlled maneuvers. The aspect of an aircraft control system which concerns these cues is called control loading.

One objective of an aircraft flight simulator is to familiarize pilots with the control forces required to perform well-executed maneuvers. Thus, the control loading system in an aircraft simulator must be capable of accurately reproducing force cues typical of the real aircraft. Most simulator control loading systems in current use consist of an electrohydraulic position servo driven by an analog computer, which can generally be programed to simulate a wide spectrum of aircraft characteristics.

The requirement of fast response over a wide performance range, together with inertial and elastic effects in the control linkage, can cause unsatisfactory performance of

*Assistant Professor of Mechanical Engineering, Iowa State University of Science and Technology, Ames, Iowa.

a control loading system in some ranges of operation. The purpose of this study was to examine a particular wide-range control loading system in order to determine the causes of unsatisfactory performance and to devise an alternative control scheme which would improve the behavior of the system over the specified range of operation.

The problem was attacked in two phases. The analysis phase of the study was needed to determine the dynamic characteristics of the fixed components of the system, that is, the plant. Prior experimental data showed that there was an undesirable low frequency oscillation in the elevator system which could not be attributed to known elements of the system. The hypothesis of mechanical compliance in the control linkage was substantiated by comparing the behavior of a mathematical model of the system with previously obtained experimental data.

The design of an alternative control scheme commenced when the mathematical model of the fixed plant, including linkage compliance, was judged to be capable of satisfactorily predicting the behavior of the real plant. The form of the proposed compensation was computed by use of a dynamic programing algorithm and a linear state space model of the plant. Input and feedback control coefficients were obtained for the entire simulation range of the system by minimizing a quadratic cost index. Behavior of the closed-loop system, as predicted by the revised mathematical model, indicated that the low frequency structural oscillation can be reduced. The compensated system was shown to be relatively insensitive to variations in the control coefficients, and certain feedback paths could be eliminated without seriously degrading the performance of the system. The revised model indicates that the control scheme is physically feasible.

SYMBOLS

Values are given in both SI Units and U.S. Customary Units; the measurements and calculations were made in U.S. Customary Units.

A	cross-sectional area of actuator piston, cm^2 (in^2)
B	modeled damping coefficient, N-cm-sec (lb-in-sec)
c	damping coefficient of linkage, N-sec/cm (lb-sec/in.)
$\bar{c}$	control coefficient vector
$c_1, c_2, \ldots, c_7$	components of control coefficient vector
C_i	valve current gain, cm^3/sec-mA (in^3/sec-mA)

C_p	valve pressure gain, $cm^5/N\text{-}sec$ $(in^5/lb\text{-}sec)$
e	plant-input control variable, V
e_F	output of load cell circuit, V
e_P	output of potentiometer circuit, V
e_T	input test signal, V
F_c	load cell force, N (lb)
F_p	pilot input force, N (lb)
G	modeled spring rate, N-cm/rad (lb-in/rad)
G_{max}	maximum value of modeled spring rate, N-cm/rad (lb-in/rad)
i	current, mA
i_r	rated valve current, mA
I	modeled control inertia, $N\text{-}cm\text{-}sec^2$ $(lb\text{-}in\text{-}sec^2)$
J	mass moment of inertia of column, $N\text{-}cm\text{-}sec^2$ $(lb\text{-}in\text{-}sec^2)$
k	spring rate of linkage, N/cm (lb/in.)
K_1	transducer gain, V/N (V/lb)
K_2	admittance of valve circuit, mA/V
K_3	gain of potentiometer circuit, V/cm (V/in.)
l_1	distance between link attachments on bellcrank, cm (in.)
l_2	distance between piston link attachment and bellcrank pivot, cm (in.)
p	load pressure, N/cm^2 (lb/in^2)

p_1 pressure on side 1 of piston, N/cm^2 (lb/in^2)

p_2 pressure on side 2 of piston, N/cm^2 (lb/in^2)

p_r valve return pressure, N/cm^2 (lb/in^2)

p_s valve supply pressure, N/cm^2 (lb/in^2)

q fluid flow rate, cm^3/sec (in^3/sec)

q_i component of linearized valve flow rate, cm^3/sec (in^3/sec)

q_r rated valve flow rate, cm^3/sec (in^3/sec)

R_1, R_2 weighting factors

R_b lever arm of column base, cm (in.)

R_p lever arm of pilot force, cm (in.)

t time, sec

T column torque, N-cm (lb-in.)

$\bar{u}$ input vector

V performance index

V_E effective volume of compressed fluid, cm^3 (in^3)

$\bar{x}$ state vector

x_b displacement of column base, cm (in.)

x_p displacement of actuator piston, cm (in.)

$\bar{y}$ output vector

$[A], [B], [C], [D], [E]$ matrices

$[H]$ input transition matrix, $\left([\Phi] - [I]\right)[A]^{-1}[B]$

$[I]$ identity matrix

$[Q]$ weighting matrix

$[\Phi]$ state transition matrix, $[e^{At}]$

α linkage ratio, $\frac{l_2}{l_1 + l_2}$

β bulk modulus of elasticity of fluid, N/cm^2 (lb/in^2)

δ voltage corresponding to desired column displacement, V

ζ valve damping ratio

θ angular displacement of column, rad

ω_n natural frequency of valve, rad/sec

Superscripts:

T transpose

-1 inverse

* nominal value

. first derivative with respect to time

.. second derivative with respect to time

Subscript:

j integer

DEVELOPMENT OF MATHEMATICAL MODEL

A complete aircraft simulator control loading system includes systems which provide force cues in the elevator, aileron, and rudder control modes; however, only an elevator system is considered here. Ordinarily, although elevator, aileron, and rudder systems are independent of one another, they are similarly structured and, therefore, an analysis of the elevator system would be applicable to aileron and rudder systems with slight modifications. In addition, the pilot control elements associated with the elevator system vary from one aircraft to another more widely than do the similar elements for the aileron and rudder systems; consequently, the elevator system would represent the loading mode most likely to present difficulties in the design of a wide-range simulation system.

The elevator control loading system examined here is shown in mechanical schematic form in figure 1. The control loading system senses the pilot input force by means of a load cell in the actuator-column linkage and transmits an electrical signal e_F to the computer which in turn commands the positioning system. The difference between the computer output and the position feedback e_P controls the fluid flow and thereby the motion of the control column. The computer can be programed to provide a wide range of dynamic characteristics typical of control loads which occur in real aircraft; however, programable nonlinear effects, such as breakout, hysteresis, and velocity limiting, are not considered herein.

As figure 1 indicates, the control loading system comprises a doubly closed-loop system whose input force and output position are transmitted through the same element, that is, the pilot's control column. Ideally the inner loop, which contains the servovalve and actuator, should have a fairly flat frequency response over a wide bandwidth. Rapid response is desired, but a change in phase margin must be made to provide stability when the outer loop is closed. Thus, the inner loop (hydraulic servo) is designed to be somewhat overdamped. A development of the mathematical model of the original system follows.

Hydraulic Servo Model

The principal components of the hydraulic servo are the amplifier, valve, actuator, load, and position transducer. The amplifier is assumed to have sufficient bandwidth to be considered a constant multiplier whose input is a voltage signal and whose output is a valve current. The servovalve is a four-way, two-stage electrohydraulic control valve whose input is a current signal and whose output is a fluid flow rate through the actuator. The static flow-pressure characteristics of the valve are essentially parabolic, typical of orifice flow-pressure relations (ref. 1). This relationship

$$q = \frac{q_r}{i_r} i \sqrt{\frac{p_s - p}{p_s}} \tag{1}$$

which is illustrated in figure 2, may be linearized about a nominal operating point through the use of a modified Taylor's series (ref. 2) as follows:

$$q = C_i i - C_p p \tag{2}$$

where

$$C_i = \left.\frac{\partial q}{\partial i}\right|_{\substack{i=i^* \\ p=p^*}}$$

$$C_p = -\left.\frac{\partial q}{\partial p}\right|_{\substack{i=i^* \\ p=p^*}}$$

and i^* and p^* are the valve current and load pressure at the nominal operating point. In this model, i^* was chosen to be 20 percent of rated current and p^* was chosen to be 33 percent of supply pressure. Servovalve frequency response (that is, the ratio of load flow with zero load pressure drop to input current) was assumed to be similar to a linear second-order system with a natural frequency of 60 Hz and damping ratio of 0.9 (ref. 3). The resulting equations describing the dynamic behavior of the servovalve are

$$\ddot{q}_i + 2\zeta\omega_n\dot{q}_i + \omega_n{}^2 q_i = C_i\omega_n{}^2 i \tag{3}$$

and

$$q = q_i - C_p p \tag{4}$$

Thus, the flow to the actuator is expressed as a sum of linear terms in control current and load pressure.

The dynamic equation governing the motion of the actuator can be determined by considering the flow continuity equation (ref. 1) or

$$q = A\dot{x}_p + \left(V_E/4\beta\right)\dot{p} \tag{5}$$

Although leakage between the piston and cylinder is often included in continuity equations for actuators, it is neglected in this analysis because the actuator piston seal in this system reduces leakage flow to an extremely small fraction of displacement and compressibility flows.

Load and Linkage Dynamics

A peculiar characteristic of a simulator control loading system is that the input and output elements are one and the same. The pilot input to the system is a force applied to the control column, and the output is the angular displacement of the column. A schematic diagram of this input-output arrangement is shown in figure 3. Two models will be formulated: (1) a rigid model based upon the assumption that all elements of the linkage and supporting structures are rigid, and (2) a compliant model based upon the assumption that the input-output linkage contains flexible elements which may be considered as one member in the analysis.

Rigid linkage model.- The equation for the motion of the actuator piston and control column may be formulated by applying Newton's second law to a free-body representation of the control column. The torques about the pivot point of the column (see fig. 3) are summed to give

$$\sum T = R_p F_p + \alpha R_b A p = J\ddot{\theta} \tag{6}$$

From the geometry of the column, $\theta = x_b/R_b$ (for small motions), where x_b is the linear displacement of the base of the column. Thus, equation (6) may be written as

$$\ddot{x}_b = \left(\alpha R_b{}^2 A/J\right)p + \left(R_b R_p/J\right)F_p \tag{7}$$

Expressed in terms of the actuator displacement x_p, equation (7) becomes

$$\ddot{x}_p = \left(\alpha^2 R_b{}^2 A/J\right)p + \left(\alpha R_b R_p/J\right)F_p \tag{8}$$

The mass of the actuator piston and load cell is assumed to be negligible compared to the inertia of the column.

Compliant linkage model.- The dynamic equations which describe the motion of the actuator piston and control column can be determined from a free-body representation of the load cell attached to the actuator output. In this case, the linkage is assumed to contain flexible elements, and the dynamic properties may be contained in the linkage member immediately connected to the load cell (see fig. 4); that is,

$$\sum F_c = Ap = k\left(x_p - \alpha x_b\right) + c\left(\dot{x}_p - \alpha \dot{x}_b\right) \tag{9}$$

Equation (9) may be arranged in the following manner:

$$\dot{x}_p = -(k/c)x_p + (A/c)p + (\alpha k/c)x_b + \alpha \dot{x}_b \tag{10}$$

Since the load cell and piston are assumed to contribute no inertial force, the equation of motion for the column is given as before by equation (7). The spring rate and damping coefficient can be computed from experimental observations of column motion and knowledge of the column inertia.

It is assumed that the displacement of the actuator piston and column can be measured directly with transducers whose dynamic contributions are negligible and also that the load cell contributes no dynamic effects.

Analog Computer

The analog computer receives force signals from the load cell and generates displacement voltages which drive the hydraulic servo. In order to reproduce the loading effects typical of a wide variety of aircraft controls, the computer may be programed to simulate a linear second-order system with variable natural frequency and damping ratio.

The dynamic equation solved by the analog computer is

$$I\ddot{\delta} + B\dot{\delta} + G\delta = T \tag{11}$$

The input and output of the analog computer are scaled voltages, proportional to the actual column torque and desired output, respectively. Accordingly, equation (11) may be written as

$$I\ddot{\delta} + B\dot{\delta} + G\delta = G_{max}K_1Ap \tag{12}$$

The hydraulic servo input is related to the analog computer output voltage by

$$i = K_2\left(\delta - K_3x_p\right) \tag{13}$$

The effect of compliance in the load linkage can now be assessed. The presence of a compliant member introduces an additional degree of freedom and associated phase lag; consequently, the rigid linkage assumption leads to incorrect predictions of system performance and inappropriate feedback policies. Inclusion of a compliant linkage mem-

ber in the mathematical model of the system enables the model to predict response phenomena similar to that observed in the laboratory. Furthermore, the hypothesis of unavoidable compliance in the control linkage provides a basis for compensation of the system.

State Vector Models

Linear state vector formulation is a convenient means by which analysis, simulation, and compensation of the control loading system may be accomplished. A typical form of these vector equations is

$$\dot{\bar{x}} = [A]\bar{x} + [B]\bar{u} \tag{14a}$$

$$\bar{y} = [C]\bar{x} + [D]\bar{u} \tag{14b}$$

where $[A]$, $[B]$, $[C]$, and $[D]$ are constant matrices.

The complete dynamic model of the control loading system with rigid control linkage is shown as a block diagram in figure 5. The numerical values used in this system are given in the appendix. The appropriate assembly of equations (3), (4), (5), (8), (12), and (13) which expresses the rigid model in the form of equations (14a) and (14b) becomes

$$\frac{d}{dt}\begin{bmatrix} x_p \\ \dot{x}_p \\ p \\ q_i \\ \dot{q}_i \\ \delta \\ \dot{\delta} \end{bmatrix} = \begin{bmatrix} 0 & 1 & 0 & 0 & 0 & 0 & 0 \\ 0 & 0 & \alpha^2 R_b{}^2 A/J & 0 & 0 & 0 & 0 \\ 0 & -4A\beta/V_E & -4\beta C_p/V_E & 4\beta/V_E & 0 & 0 & 0 \\ 0 & 0 & 0 & 0 & 1 & 0 & 0 \\ -C_i\omega_n{}^2K_2K_3 & 0 & 0 & -\omega_n{}^2 & -2\zeta\omega_n & C_i\omega_n{}^2K_2 & 0 \\ 0 & 0 & 0 & 0 & 0 & 0 & 1 \\ 0 & 0 & K_1G_{max}A/I & 0 & 0 & -G/I & -B/I \end{bmatrix} \begin{bmatrix} x_p \\ \dot{x}_p \\ p \\ q_i \\ \dot{q}_i \\ \delta \\ \dot{\delta} \end{bmatrix} + \begin{bmatrix} 0 \\ \alpha R_b R_p/J \\ 0 \\ 0 \\ 0 \\ 0 \\ 0 \end{bmatrix} F_p \tag{15}$$

$$\theta = \frac{1}{\alpha R_b} x_p \tag{16}$$

Figure 6 shows a block diagram of the model having compliant linkage. The numerical values used in this system are given in the appendix. The complete dynamic model including compliant linkage is written in state vector form by using equations (3), (4), (5), (7), (10), (12), and (13); that is,

$$\frac{d}{dt}\begin{bmatrix} x_p \\ p \\ q_i \\ \dot{q}_i \\ \delta \\ \dot{\delta} \\ x_b \\ \dot{x}_b \end{bmatrix} = \begin{bmatrix} -k/c & A/c & 0 & 0 & 0 & 0 & \alpha k/c & \alpha \\ 4A\beta k/V_E c & -4\beta\left(A^2 + C_p c\right)/V_E c & 4\beta/V_E & 0 & 0 & 0 & -4A\beta\alpha k/V_E c & -4A\beta\alpha/V_E \\ 0 & 0 & 0 & 1 & 0 & 0 & 0 & 0 \\ -C_i\omega_n{}^2K_2K_3 & 0 & -\omega_n{}^2 & -2\zeta\omega_n & C_i\omega_n{}^2K_2 & 0 & 0 & 0 \\ 0 & 0 & 0 & 0 & 0 & 1 & 0 & 0 \\ 0 & K_1G_{max}A/I & 0 & 0 & -G/I & -B/I & 0 & 0 \\ 0 & 0 & 0 & 0 & 0 & 0 & 0 & 1 \\ 0 & \alpha R_b{}^2A/J & 0 & 0 & 0 & 0 & 0 & 0 \end{bmatrix} \begin{bmatrix} x_p \\ p \\ q_i \\ \dot{q}_i \\ \delta \\ \dot{\delta} \\ x_b \\ \dot{x}_b \end{bmatrix} + \begin{bmatrix} 0 \\ 0 \\ 0 \\ 0 \\ 0 \\ 0 \\ 0 \\ R_bR_p/J \end{bmatrix} F_p \qquad (17)$$

$$\theta = \frac{1}{R_b} x_b \qquad (18)$$

The input signal e_T, shown at the input to the valve amplifier in figures 5 and 6, represents a voltage signal used for obtaining system frequency response data both in the laboratory (see fig. 7) and in the mathematical models.

COMPARISON OF RIGID AND COMPLIANT MODELS

All numerical values for coefficients in the rigid linkage model were determined from component manufacturers' specifications, geometric considerations, and analytical calculations. Simulation of the system using this model revealed that such a model is incapable of predicting the low frequency resonances observed in the laboratory.

Inclusion of a compliant linkage member between the actuator piston and the control column in the mathematical model provided the means by which approximate laboratory behavior could be predicted. The linkage spring rate and damping coefficient were chosen so that the observed resonance in the hydraulic servo was matched by the mathematical model. Predicted open-loop and closed-loop servo frequency responses are shown in figures 8 and 9, respectively. Resonance peaks, which are seen to occur at approximately 12 Hz with a damping ratio of 0.1, correspond favorably with laboratory observations.

The overall system open-loop frequency response, shown in figure 10, illustrates the sizable decrease in phase margin introduced by compliance in the load linkage. This difference in phase margin is a plausible explanation for the discrepancy between behavior predicted by the rigid model and that observed in the laboratory; the closed-loop system becomes unstable for low values of computer-modeled spring rate G which correspond to high loop gain. Typical predicted closed-loop responses to step pilot forces for the rigid and compliant models can be compared in figures 11(a) and 11(b). The response of the compliant model displays the characteristics of the laboratory system and thus qualifies it for use in developing compensation for the laboratory system.

COMPENSATION OF THE SYSTEM

The problems of linkage compliance and resulting output oscillations have at least two possible solutions. One solution is the removal of sources of compliance in the linkage by altering or stiffening the linkage members, linkage bearings, and bearing mounts. This method, however, may be unsatisfactory because of additional weight or space requirements, and quite likely such a solution would, at best, elevate the structural resonance rather than eliminate its effects.

Another solution, which is developed here, considers the linkage compliance to be an inextricable component of the fixed plant. Accordingly, the compensation proposed in this section requires knowledge of the resonant frequency of the linkage. This information is obtained from the laboratory system by measuring the piston and column responses in tests of the loaded hydraulic servo.

The fixed plant, for purposes of compensation, is shown in figure 12. The plant is considered to have only one input e which drives the valve amplifier; the pilot force is represented by an additional state variable. The state equations which govern this plant are

$$\frac{d}{dt}\begin{bmatrix} x_p \\ p \\ \delta \\ \dot{\delta} \\ x_b \\ \dot{x}_b \\ F_p \end{bmatrix} = \begin{bmatrix} -k/c & A/c & 0 & 0 & \alpha k/c & \alpha & 0 \\ 4A\beta k/V_E c & -4\beta\left(A^2 + C_p c\right)/V_E c & 0 & 0 & -4A\alpha\beta k/V_E c & -4A\alpha\beta/V_E & 0 \\ 0 & 0 & 0 & 1 & 0 & 0 & 0 \\ 0 & 0 & -G/I & -B/I & 0 & 0 & G_{max}/I \\ 0 & 0 & 0 & 0 & 0 & 1 & 0 \\ 0 & \alpha R_b{}^2 A/J & 0 & 0 & 0 & 0 & R_p R_b/J \\ 0 & 0 & 0 & 0 & 0 & 0 & 0 \end{bmatrix} \begin{bmatrix} x_p \\ p \\ \delta \\ \dot{\delta} \\ x_b \\ \dot{x}_b \\ F_p \end{bmatrix} + \begin{bmatrix} 0 \\ 4\beta C_1 K_2/V_E \\ 0 \\ 0 \\ 0 \\ 0 \\ 0 \end{bmatrix} e \qquad (19)$$

In this model, the flow control valve dynamics are neglected. This approximation was found to be reasonable for design purposes and advantageous when implementation of the compensation is considered. As equation (19) shows, the pilot input force F_p can be described by the differential equation $dF_p/dt = 0$, whose solution for $F_p(0) \neq 0$ is a constant. Thus, in the compensation design procedure, F_p is a step function. Note that the analog computer is included in the plant description.

The compensation design was accomplished by computing a feedback law $e = \bar{c}^T \bar{x}$ and performance index V so that

$$V = \min_{\bar{c}} \int \left(\bar{x}^T [Q] \bar{x} + R_2 e^2 \right) dt \qquad (20)$$

where $[Q]$ is a positive definite matrix, R_2 is a positive scalar, $\bar{c}$ is a constant vector, and $\bar{x}$ is defined as in equation (19). The matrix $[Q]$ was chosen so that the quadratic term $\bar{x}^T[Q]\bar{x}$ became

$$\bar{x}^T[Q]\bar{x} = 100(\delta - \theta)^2 + R_1(\dot{\delta} - \dot{\theta})^2 \tag{21}$$

Therefore, the performance criterion was the minimum integral of the squared difference between desired and actual output displacements and velocities. The term R_2e^2 in equation (20) provides a linear limit constraint on the valve amplifier input e. The maximum magnitude of e, and hence maximum valve current and flow rate, can be controlled by adjusting the weighting factors R_1 and R_2.

The feedback coefficient vector $\bar{c}$ was computed by approximating the integral in equation (20) by a sum and applying a discrete dynamic programing algorithm (ref. 4). The numerical algorithm resulting from these operations is

$$\bar{c}_j = -\left(R_2 + [H]^T[E]_{j-1}[H]\right)^{-1}[H]^T[E]_{j-1}[\Phi] \tag{22a}$$

$$[E]_j = \left([\Phi] + [H]\bar{c}_j\right)^T[E]_{j-1}\left([\Phi] + [H]\bar{c}_j\right) + [Q] + \bar{c}_j{}^T R_2 \bar{c}_j \tag{22b}$$

The determination of the optimal feedback $\bar{c}$ is accomplished by assuming that $[E]_0 = [Q]$ and then recursively computing $[E]$ and $\bar{c}$ until the difference $\bar{c}_j - \bar{c}_{j-1}$ is arbitrarily small. The weighting factors R_1 and R_2 must be chosen so that the actual plant output is satisfactory (in terms of comparison with desired output) and consistent with the physical limitations of the plant components. The fidelity of the actual output ordinarily improves as the constraints on the plant are relaxed. In the system considered here, the constraint parameters R_1 and R_2 are chosen so that the column motion θ is qualitatively close to the desired motion δ for the current and flow rate limits of the flow control valve.

A diagram of the structure of the compensated system is shown in figure 13. Typical predicted responses of the compensated system are shown in figure 14, and the numerical values chosen in the compensation of the system are given in the appendix. The responses were simulated by use of the original eighth-order compliant model or equa-

tion (17) with feedback from the six state variables included in equation (19). Omission of valve dynamics in the compensation procedure did not affect the validity of the feedback law and, consequently, it is not necessary to be able to measure the fluid flow rate q and its derivative $\dot{q}$ for effective control of the system. Computed values of the feedback gains $\bar{c}$ appear to be reasonable for implementation purposes. All the six state variables in equation (19) may be measured and conditioned by conventional transducers and associated equipment. Adjustments of the feedback gains for variations in analog computer settings are required for only the computer output δ and its derivative $\dot{\delta}$. These adjustments can be accomplished by manipulating input and output gains in the computer. The compensated system model demonstrates fidelity over a wide range of computer settings and, most notably, eliminates the instability associated with low values of the modeled spring rate. A set of typical system parameters and feedback gains corresponding to the plant model examined herein is given in the appendix. Numerical experiments have indicated that this feedback scheme is reasonably insensitive to perturbations in plant parameters.

CONCLUDING REMARKS

A linear state space mathematical model and state feedback appear to provide satisfactory means for compensating a hydraulic control loading system containing compliance in the actuator control linkage. The resulting compensated system can be physically constructed by use of conventional components, and it can be adjusted to simulate a wide variety of real aircraft by altering input and output gains at the analog computer when aircraft parameters are programed.

Langley Research Center,
National Aeronautics and Space Administration,
Hampton, Va., October 7, 1974.

APPENDIX

NUMERICAL VALUES

Physical Constants of Model

These are the numerical values used in both the rigid and compliant (plant) models.

$A = 15.22\ cm^2$ $(2.36\ in^2)$

$B = 3434.74$ N-cm-sec (304 lb-in-sec)

$c = 28.372$ N-sec/cm (16.2016 lb-sec/in.)

$C_i = 89.309\ cm^3/sec\text{-}mA$ $(5.45\ in^3/sec\text{-}mA)$

$C_p = 0.24243\ cm^5/N\text{-}sec$ $(0.0102\ in^5/lb\text{-}sec)$

$F_p = 427$ N (96 lb)

$G = 108\ 466$ N-cm/rad (9600 lb-in/rad)

$G_{max} = 325\ 396$ N-cm/rad (28 800 lb-in/rad)

$i_r = 15$ mA (15 mA)

$I = 677.91\ N\text{-}cm\text{-}sec^2$ $(60\ lb\text{-}in\text{-}sec^2)$

$J = 422.56\ N\text{-}cm\text{-}sec^2$ $(37.4\ lb\text{-}in\text{-}sec^2)$

$k = 10\ 695$ N/cm (6107.86 lb/in.)

$K_1 = 0.0011240$ V/N (0.005 V/lb)

$K_2 = 1.56$ mA/V (1.56 mA/V)

$K_3 = 3.0047$ V/cm (7.632 V/in.)

$p_s = 827.28\ N/cm^2$ $(1200\ lb/in^2)$

$q_r = 1638.7\ cm^3/sec$ $(100\ in^3/sec)$

$R_b = 25.4$ cm (10 in.)

$R_p = 79.6925$ cm (31.375 in.)

$V_E = 191.73\ cm^3$ $(11.7\ in^3)$

$\alpha = 0.59$ (0.59)

$\beta = 172\ 350\ N/cm^2$ $(250\ 000\ lb/in^2)$

$\zeta = 0.9$ (0.9)

$\omega_n = 377$ rad/sec (377 rad/sec)

Compensation of the Plant

These are the numerical values chosen in the compensation of the plant.

The following values of $[Q]$ and R_2 were used for computing feedback coefficients according to equation (20):

$$[Q] = \begin{bmatrix} 0 & 0 & 0 & 0 & 0 & 0 & 0 \\ 0 & 0 & 0 & 0 & 0 & 0 & 0 \\ 0 & 0 & 100 & 0 & -10 & 0 & 0 \\ 0 & 0 & 0 & 0 & 0 & 0 & 0 \\ 0 & 0 & -10 & 0 & 1 & 0 & 0 \\ 0 & 0 & 0 & 0 & 0 & 0 & 0 \\ 0 & 0 & 0 & 0 & 0 & 0 & 0 \end{bmatrix} \qquad R_2 = 0.1$$

This $[Q]$ corresponds to $R_1 = 0$ in equation (21).

Figures 10, 11, and 14 show typical frequency and time responses associated with computer settings for a 2.0 hertz, 0.2 damped response of the control column. The feedback coefficient vector $\bar{c}$ computed from equation (20), using the values given for $[Q]$ and R_2, is given in S.I. Units as

$$\bar{c} = \begin{bmatrix} -1.94 \text{ V/cm} \\ -0.0000377 \text{ V-cm}^2\text{/N} \\ +22.02 \text{ V/V} \\ +0.669 \text{ V-sec/V} \\ +0.199 \text{ V/cm} \\ -0.00708 \text{ V-sec/cm} \\ -0.00146 \text{ V/N} \end{bmatrix}$$

and in U.S. Customary Units as

$$\bar{c} = \begin{bmatrix} -4.93 \text{ V/in.} \\ -0.000026 \text{ V-in}^2\text{/lb} \\ +22.02 \text{ V/V} \\ +0.669 \text{ V-sec/V} \\ +0.506 \text{ V/in.} \\ -0.018 \text{ V-sec/in.} \\ -0.0065 \text{ V/lb} \end{bmatrix}$$

REFERENCES

1. Merritt, Herbert E.: Hydraulic Control Systems. John Wiley & Sons, Inc., c.1967.

2. Glickman, Myron: Simulation of the Effects of Load on Hydraulic Servo Actuators. Simulation, vol. 12, no. 3, Mar. 1969, pp. 145-151.

3. Anon.: Series 72 and 73 Flow Control Servovalves. Catalog 720/730, Industrial Div., Moog Inc.

4. Noton, A. R. M.: Introduction to Variational Methods in Control Engineering. Pergamon Press, Inc., c.1965.

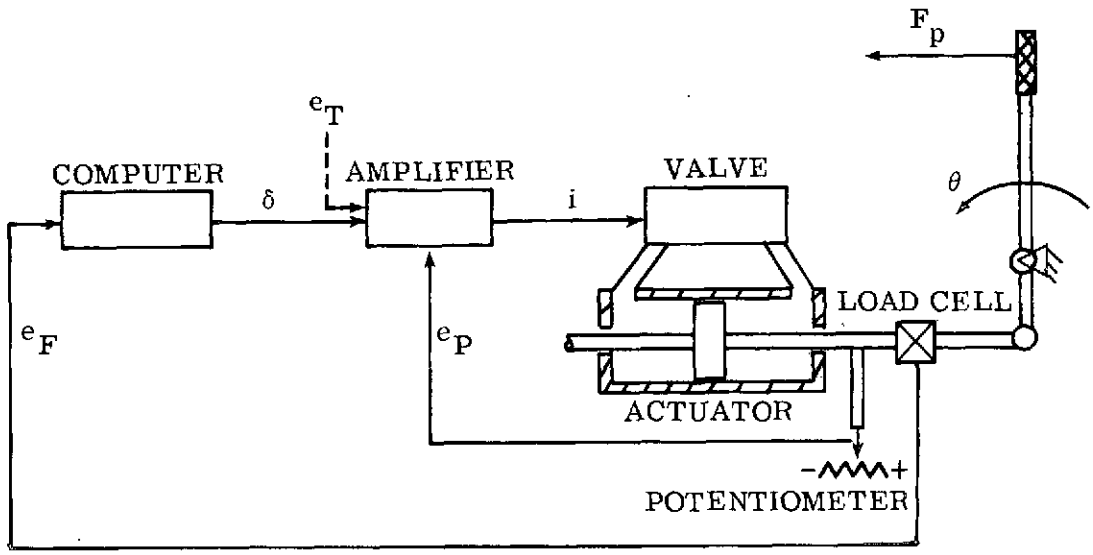

Figure 1.- Electrohydraulic control loading system.

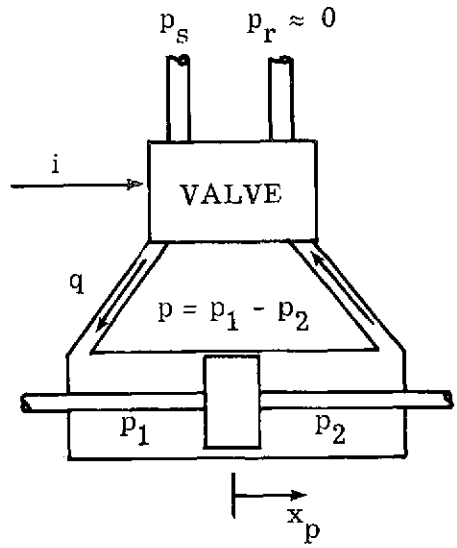

Figure 2.- Control valve and actuator.

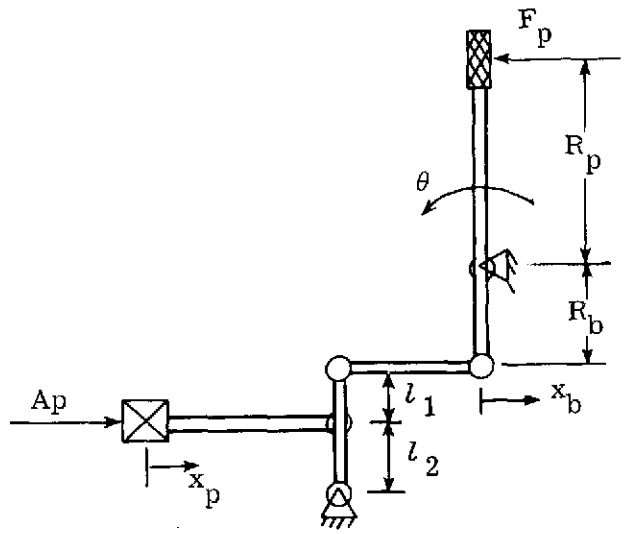

Figure 3.- Rigid input-output linkage model.

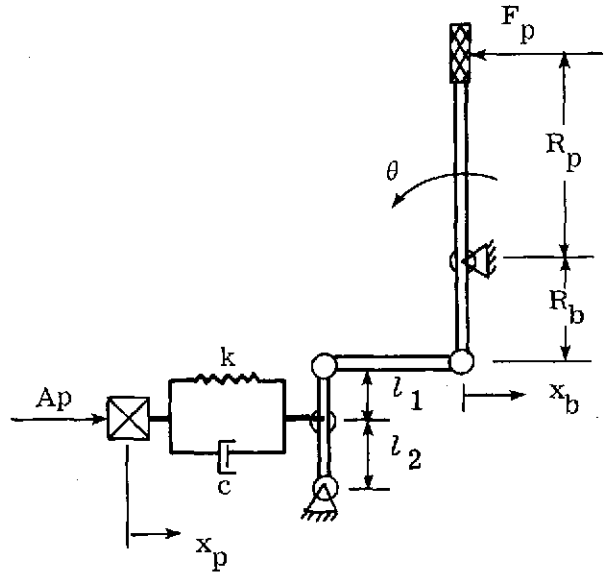

Figure 4.- Compliant input-output linkage model.

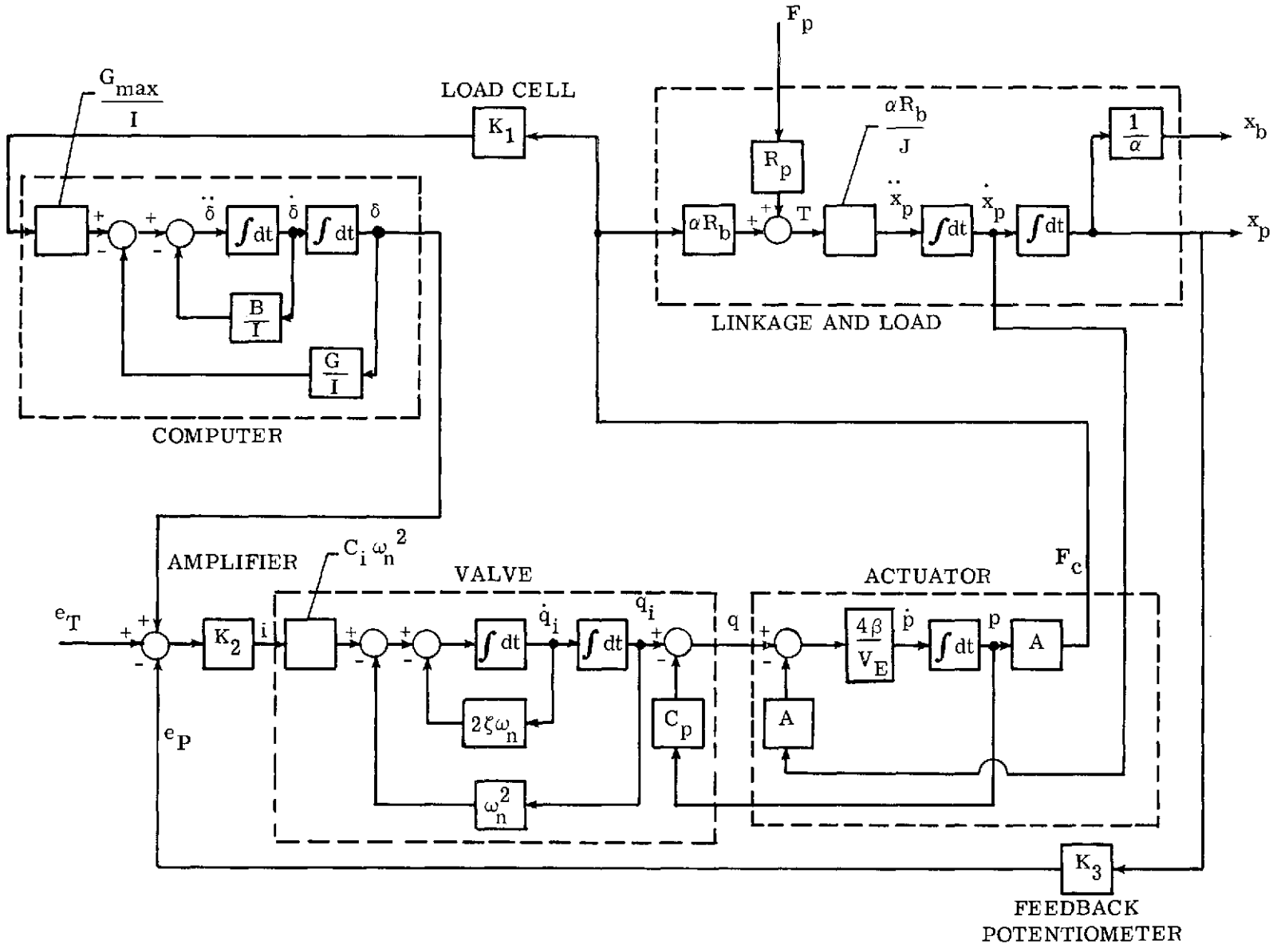

Figure 5.- Control loading system with rigid load linkage.

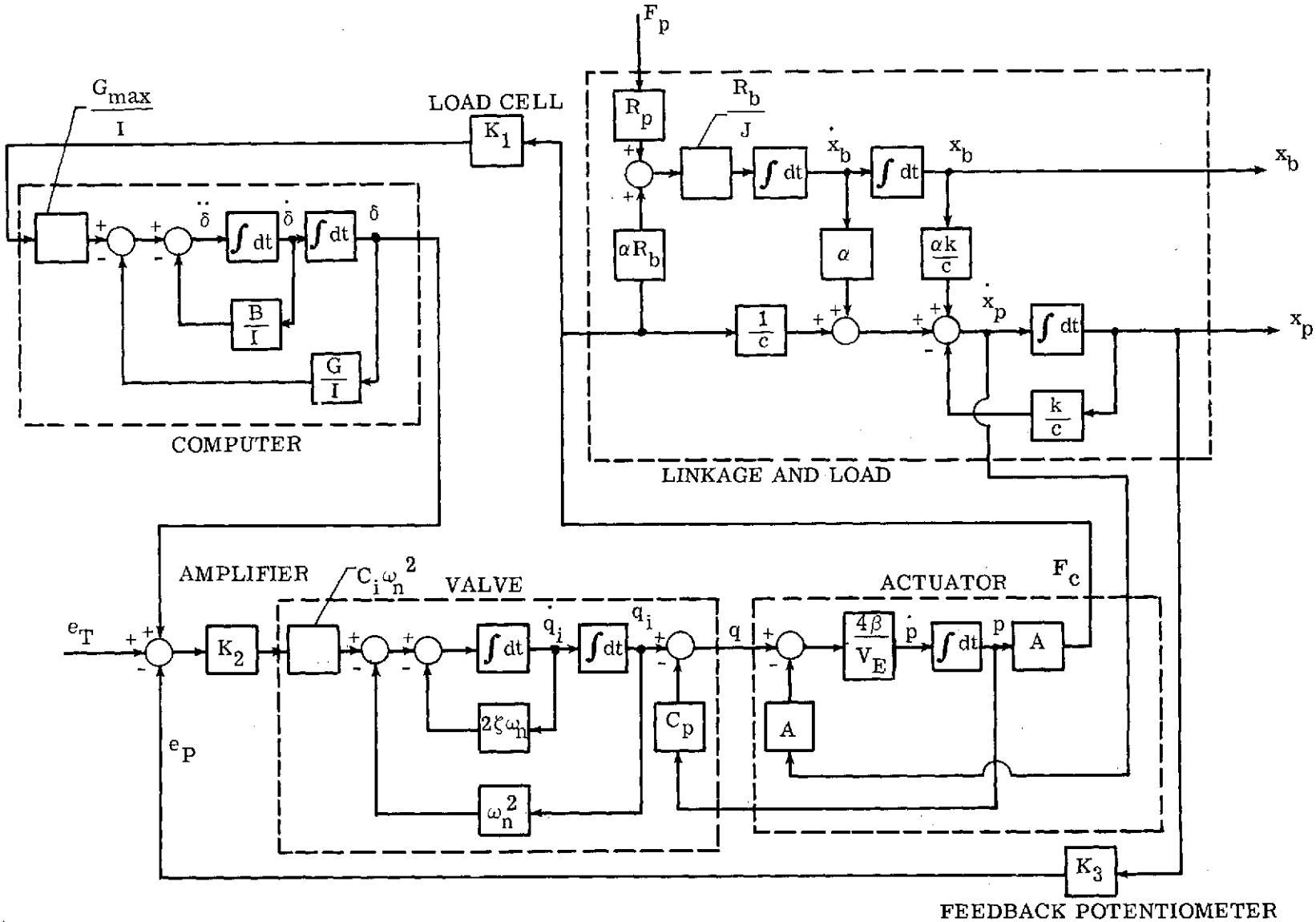

Figure 6.- Control loading system with compliant load linkage.

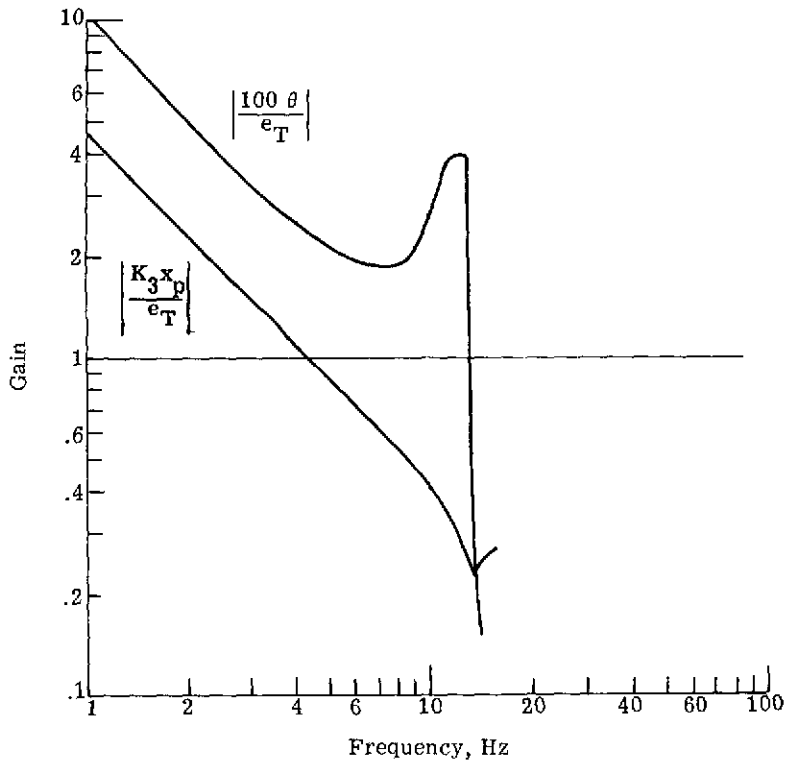

(a) Gain.

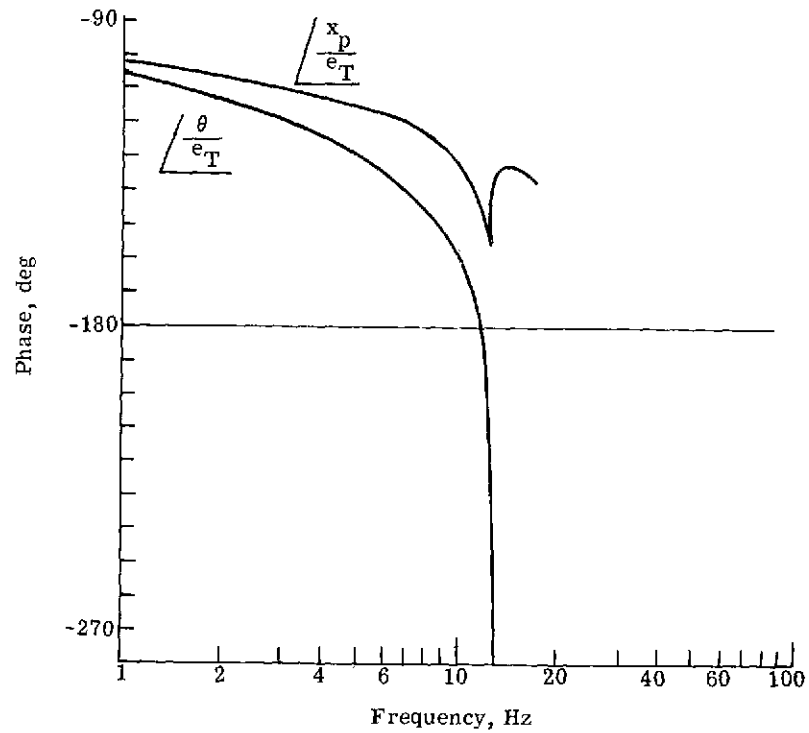

(b) Phase.

Figure 7.- Open-loop frequency response from experimental data.

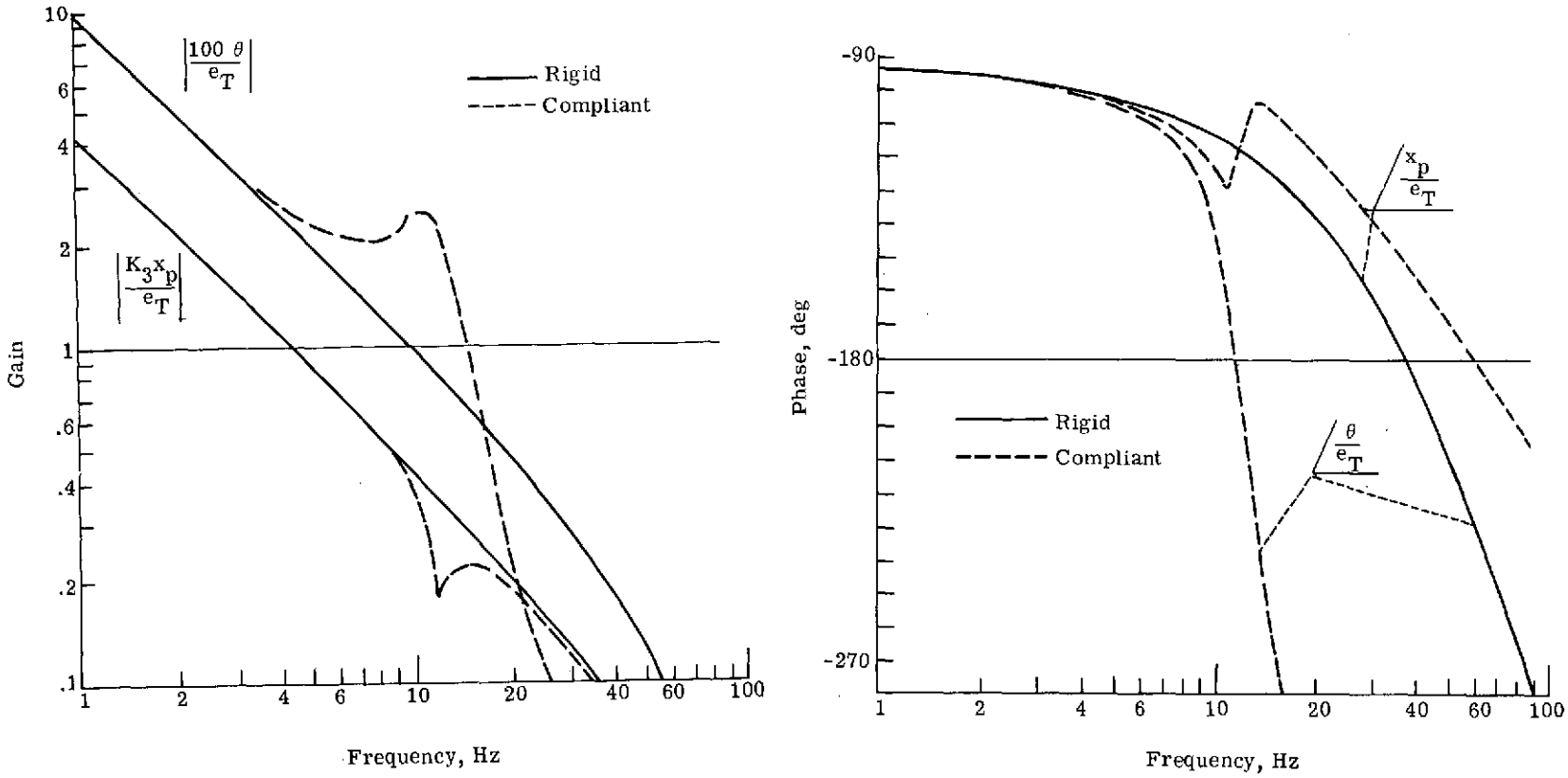

(a) Gain.

(b) Phase.

Figure 8.- Open-loop servo frequency response.

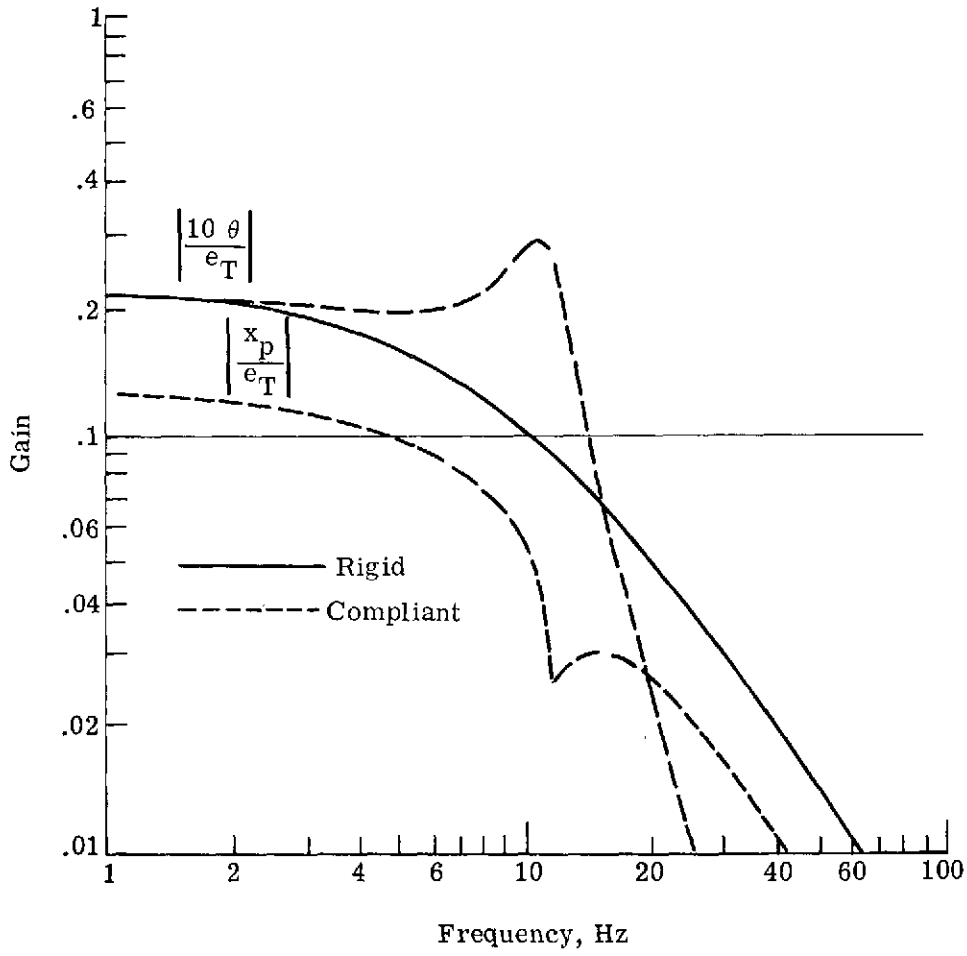

Figure 9.- Closed-loop servo frequency response.

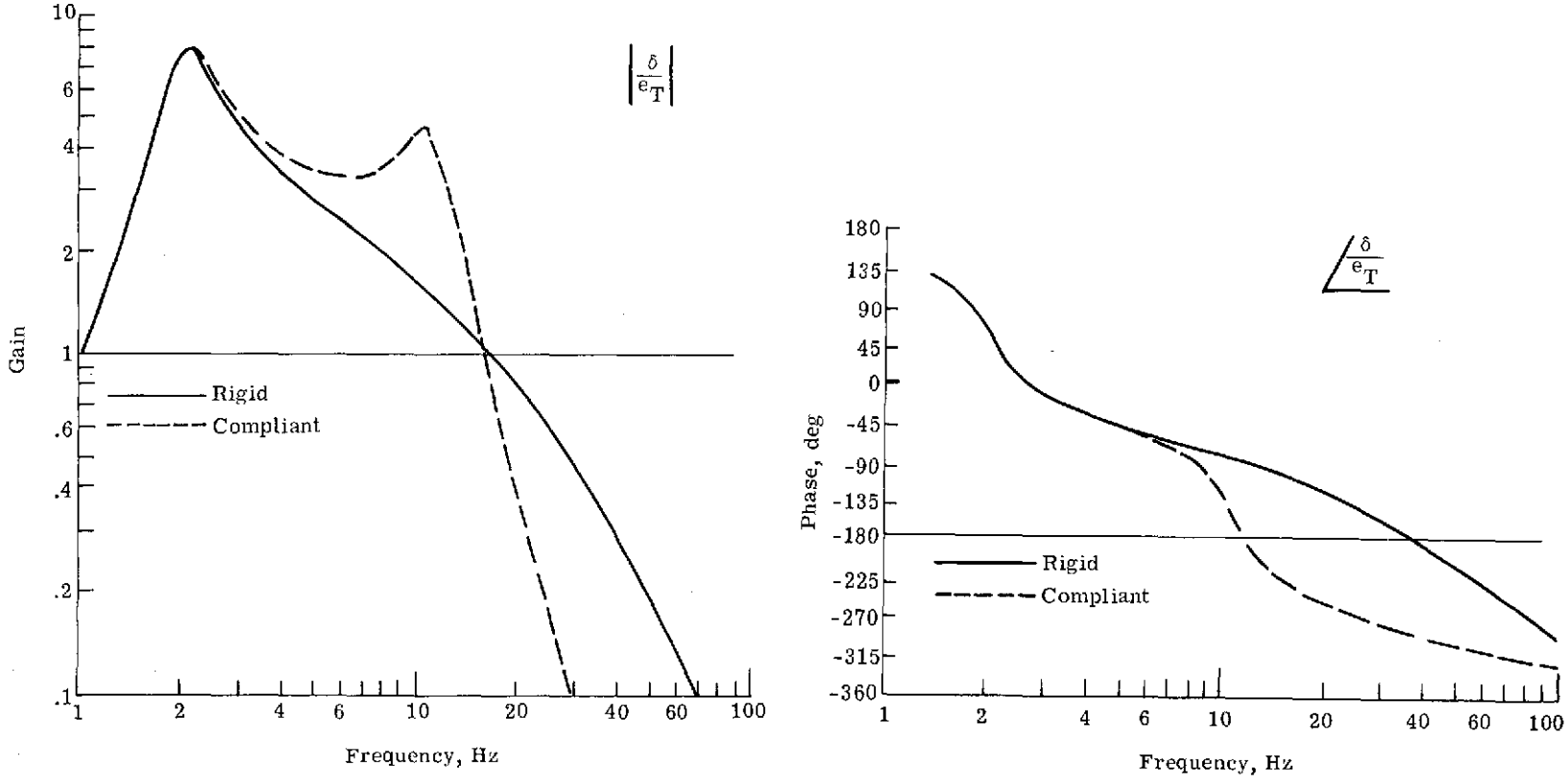

(a) Gain.

(b) Phase.

Figure 10.- Overall system open-loop frequency response. I = 67.79 N-cm-sec^2 (6 lb-in-sec^2); B = 343.47 N-cm-sec (30.4 lb-in-sec); G = 10 847 N-cm/rad (960 lb-in/rad).

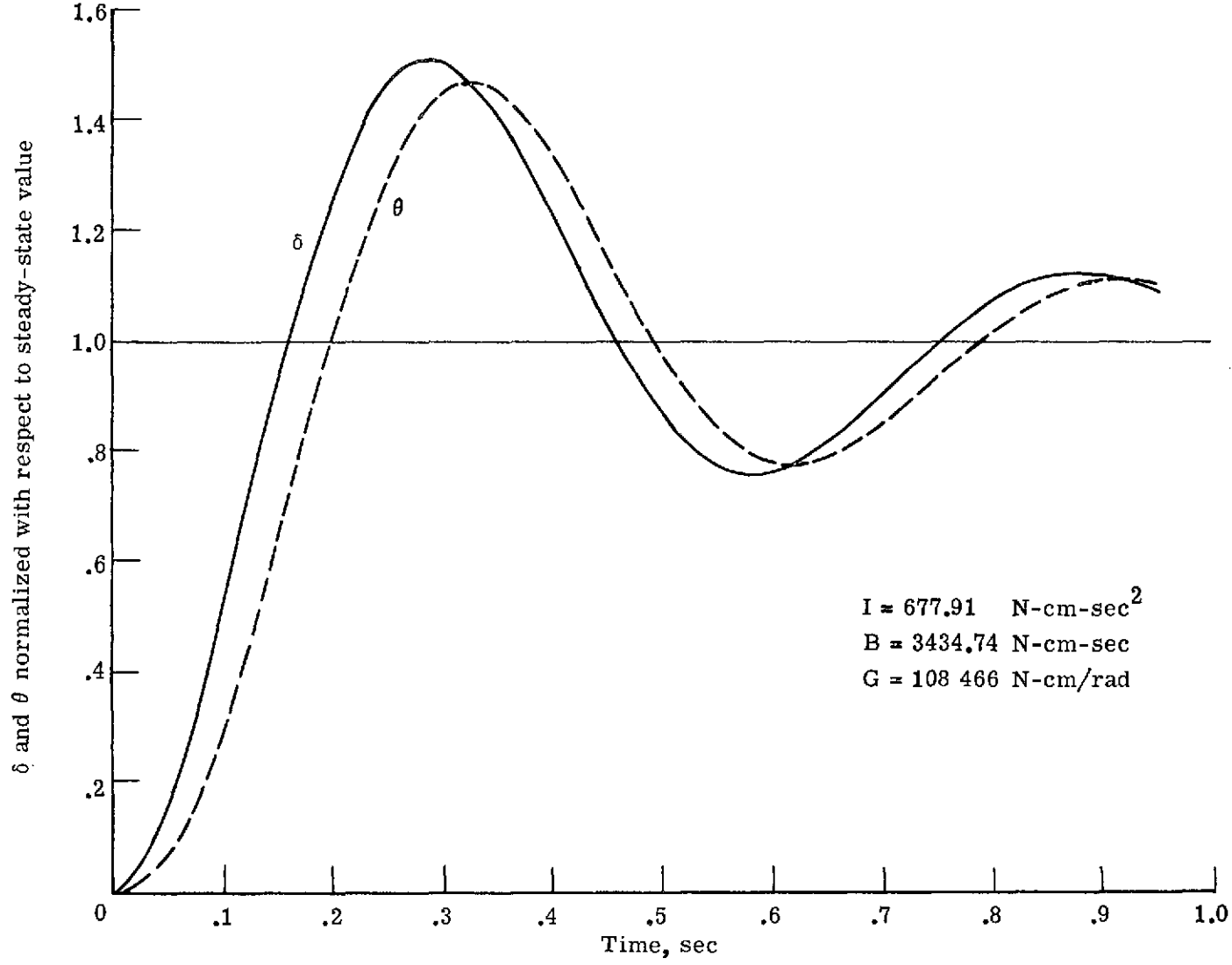

(a) Rigid model.

Figure 11.- Time response to step force input.

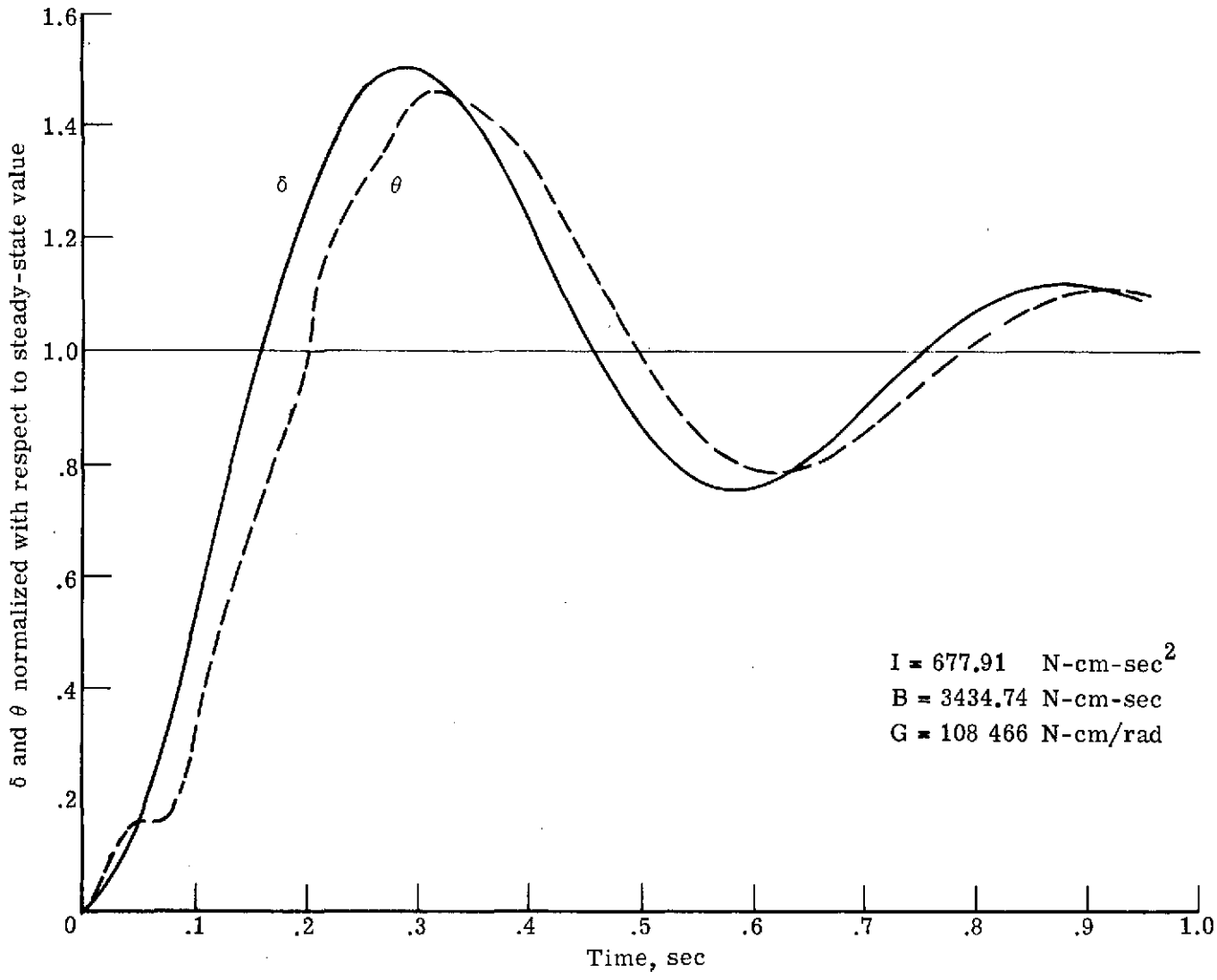

(b) Compliant model.

Figure 11.- Concluded.

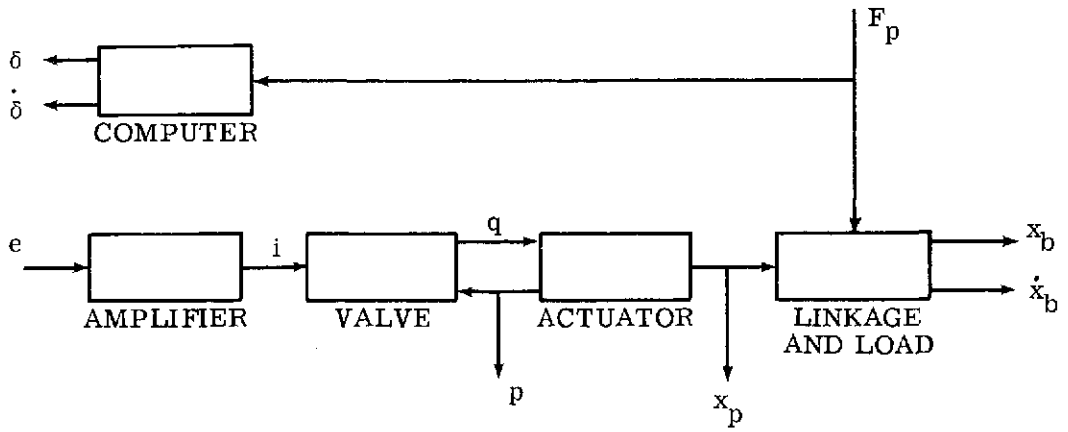

Figure 12.- Fixed plant.

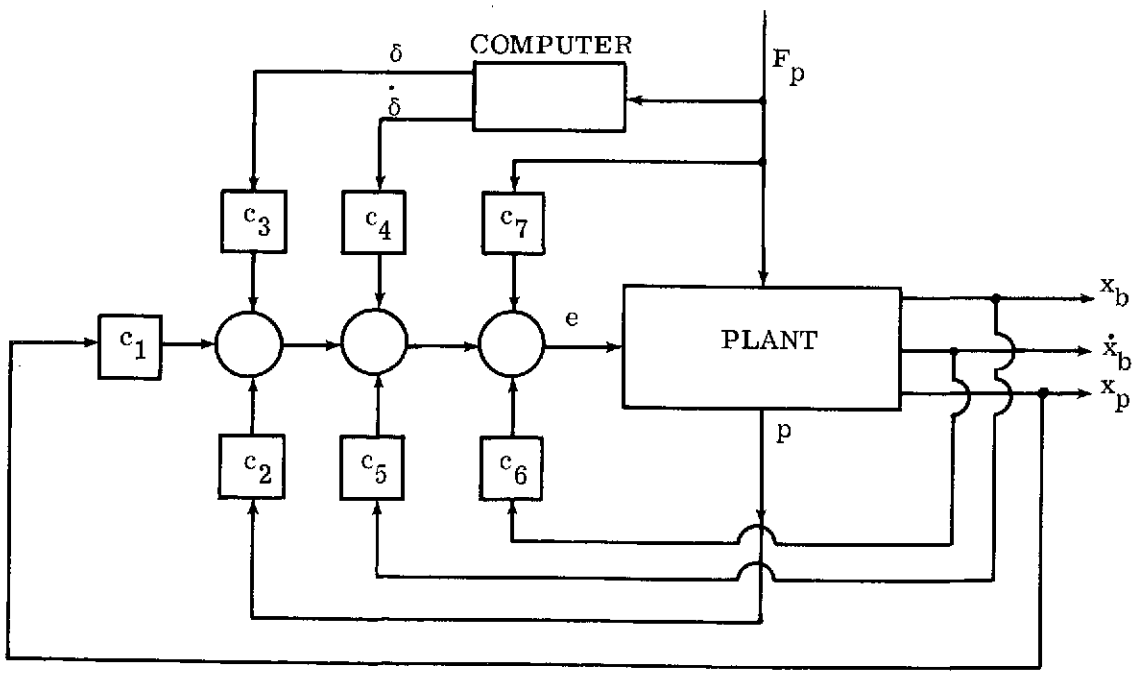

Figure 13.- Compensated system.

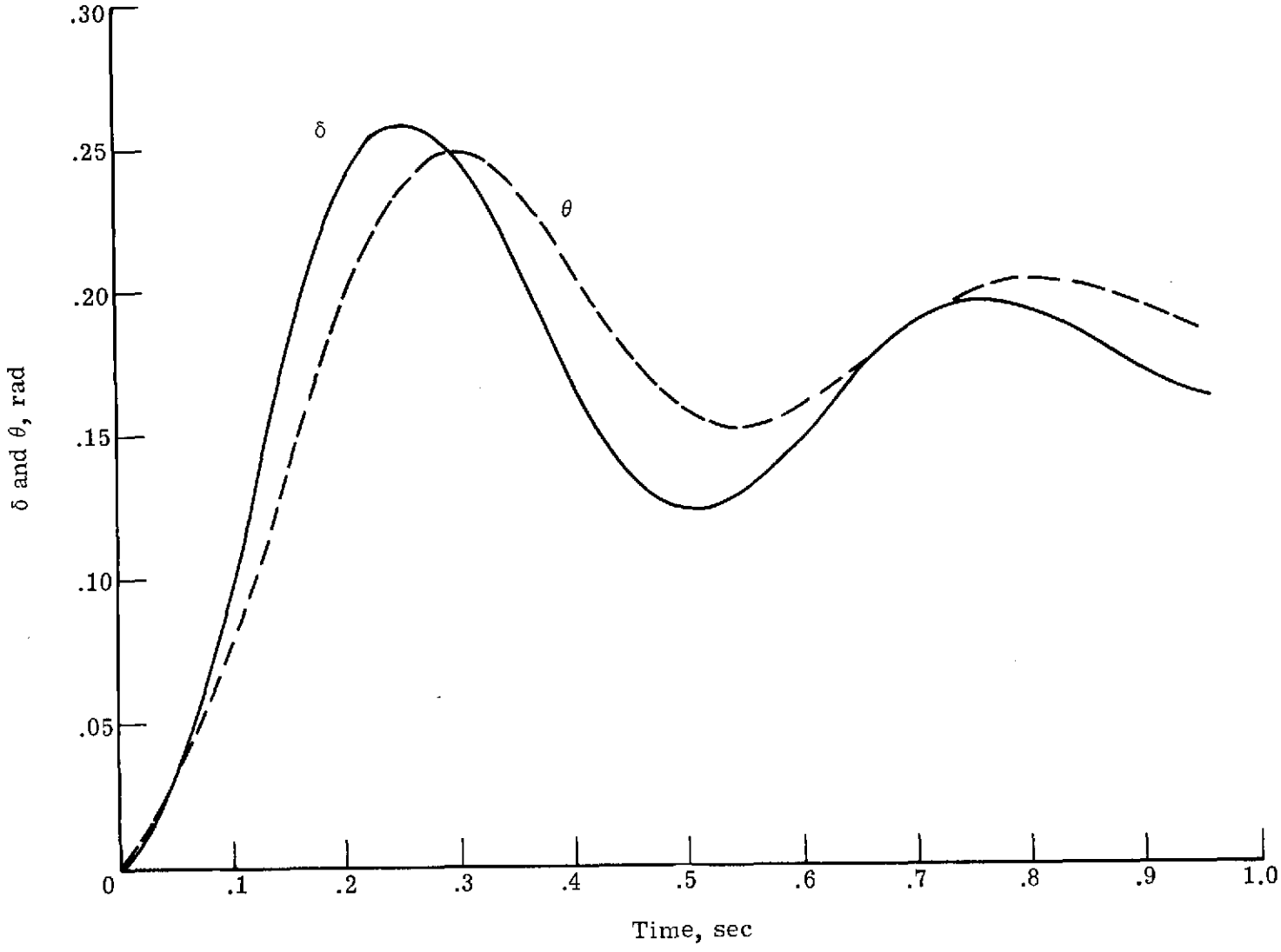

Figure 14.- Time response to step force input for compensated system. I = 677.91 N-cm-sec^2 (60 lb-in-sec^2); B = 3434.74 N-cm-sec (304 lb-in-sec); G = 108 466 N-cm/rad (9600 lb-in/rad).